

# Nucleotide-Based Elemental Mass Probes for High-Sensitive Single-Cell Mass Cytometry

Weiliang Liu, Zhian Hu,\* Wencan Jiang, Jinhui Liu, Gongwei Sun,\* Sichun Zhang,\* and Xinrong Zhang

Cite This: <https://doi.org/10.1021/acs.analchem.5c01011>

Read Online

ACCESS |



Metrics &amp; More

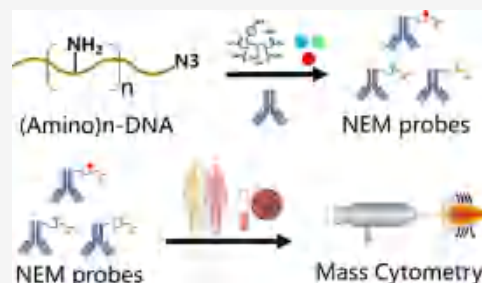


Article Recommendations



Supporting Information

**ABSTRACT:** Mass cytometry is one of the most powerful strategies for multiplexed cell-surface protein profiling and cell typing. However, its potential in cell classification is constrained by the lack of elemental mass probes. In this work, we constructed a novel nucleotide-based elemental mass probe. This probe employs nucleotide chains as its backbone and utilizes the active amino groups in the chains to couple with metal chelates, which enables it to exhibit improved sensitivity, water solubility, and biocompatibility. We applied the probes in mass cytometry analysis using a cell mixture and human peripheral blood mononuclear cells (PBMCs). The results showed that the signal-to-noise ratio of the probes is twice that of the commercial probes, and it can successfully identify the CD markers from patients' PBMCs. We hold a belief that this probe has a strong potential for clinical diagnosis and is expected to drive advancements in multiplexed cell analysis.



## INTRODUCTION

Mass cytometry (CyTOF) is a powerful tool for life science research<sup>1–3</sup> because it can measure over 100 parameters simultaneously on a single cell<sup>4,5</sup> and has been widely applied in the identification of cellular heterogeneity, drug discovery,<sup>6–8</sup> and advancing biomedical research.<sup>9–11</sup> The core reagent of CyTOF is the metal ion-tagged antibodies, that is, the mass probes. Currently, the commercial mass probe used in mass cytometry is the polymer mass probe.<sup>12</sup> This probe used the polymer backbone tags to load metal ions, and each probe can load about 150 metal ions. Due to the water solubility of the polymer decreasing significantly as the length of the chain increased, it was difficult to load more metal ions on a single probe, which limited its improvement in sensitivity.<sup>13,14</sup> To improve the mass probe's sensitivity, several nanoparticle (NP)-based mass probes have been developed, such as gold nanoparticles,<sup>15</sup> quantum dots (QDots),<sup>16,17</sup> polymer dots (Pdots),<sup>18</sup> lanthanide nanoparticles (LnNPs),<sup>19,20</sup> and zirconium-containing metal–organic framework nanoparticles (Zr-nMOFs).<sup>21</sup> The NP mass probe can load more than 10<sup>3</sup> metal ions and, thus, give a higher signal intensity. However, the nonspecific adsorption and endocytosis result in a very high background signal.<sup>22</sup> Besides, the poor stability of the NPs in phosphate-based biological buffer and the limited types of metal ions have also restricted their applications.

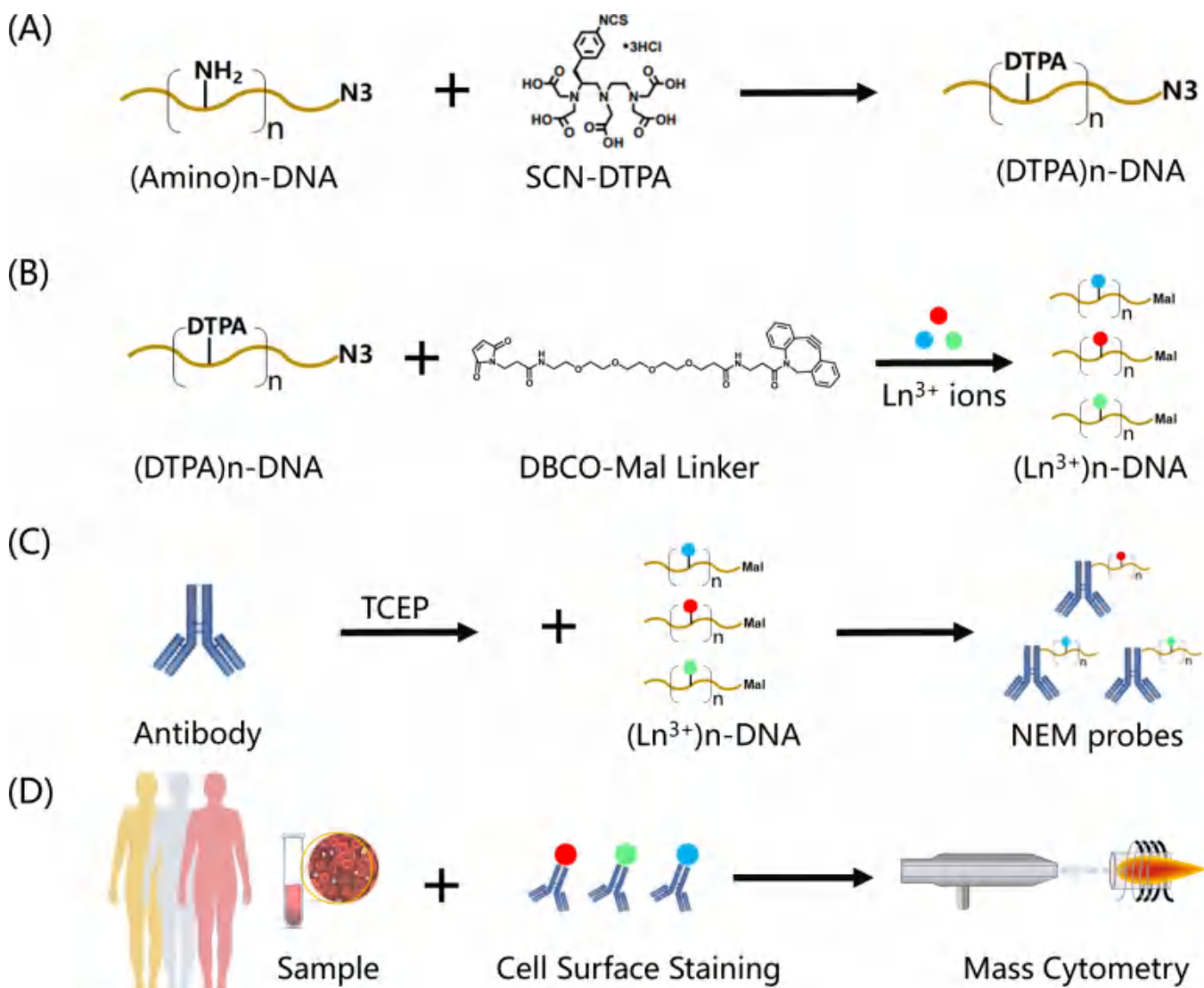
An excellent mass probe should possess the following characteristics: (1) it should have good uniformity and the number of metal ions loaded by each probe should be relatively stable; (2) the probe should possess good water solubility and biocompatibility; and (3) it can be produced in large quantities within a short time. Based on the above concepts, our group selected the double-strand DNA as the

tag's backbone and developed a DNA elemental mass tag by utilizing polymerase chain reaction (PCR).<sup>23</sup> As a natural biomolecule, DNA has a linear and flexible backbone structure like that of polymer molecules. On the other hand, it exhibits excellent water solubility and biocompatibility. Therefore, increasing its sequence length will not deteriorate its water solubility. What's more, the DNA sequence can be precisely controlled through the design of PCR templates and thus ensures its uniformity. By incorporating dNTPs with active groups (e.g., alkynyl groups) during the PCR reaction, metal-DOTA complexes can be easily labeled on the alkynyl-modified DNA backbone through click chemistry reactions. This double-stranded DNA mass tag has been successfully applied in immunoassays. However, there are still some challenges that must be overcome in mass cytometry analysis. For example, the molecular weight of the double-stranded DNA mass tag is almost comparable to that of the antibody, which makes it difficult to separate the excess DNA mass tags in the antibody labeling step. The nonspecific adsorption during the cell labeling steps leads to a high background signal. When reducing the length of the DNA sequence, the high proportion of amino-modified bases in the DNA sequence will affect the activity of DNA polymerase and the hybridization efficiency of the primers, making it difficult to prepare the

**Received:** February 16, 2025

**Revised:** May 25, 2025

**Accepted:** May 28, 2025

Scheme 1. Diagram of the Synthesis and Cell Staining of NEM Probes for Mass Cytometry<sup>a</sup>

<sup>a</sup>(A) Conjugating the (amino)*n*-DNA with SCN-DTPA. (B) Loading (DTPA)*n*-DNA with lanthanide elements and DBCO-Mal linker. (C) Labeling antibodies with (Ln<sup>3+</sup>)*n*-DNA tags. (D) Staining the cells with NEM probes and analyzed by mass cytometry

double-stranded DNA tags in a short time, even causing the PCR reaction to stop. In addition, the PCR method is not suitable for the industrial-scale preparation of DNA mass tags in large quantities.

In this work, we develop a novel nucleotide-based element mass (NEM) probe with solid-phase synthesis. Solid-phase synthesis facilitates the rapid production of large quantities of single-stranded DNA tags with lower molecular weights, thereby overcoming the separation problem of excess DNA tags in the probe purification steps. Additionally, we optimized washing buffers to solve the adsorption issues during the cell-staining process. We evaluated the potential of NEM probes in profiling cell-surface proteins in a cell mixture and PBMCs, and it shows improved performance compared with the commercially available counterparts. The NEM probe was also successfully applied to identify the CD markers in PBMCs from patients with different diseases. These results show that NEM probes can expand the current toolkits for mass cytometry.

## EXPERIMENTAL SECTION

**Loading (Amino)*n*-DNA with Lanthanide Elements and DBCO-Mal Linker.** The (amino)*n*-DNA oligonucleotides that are enriched with amino modifications were synthesized by Accurate Biotechnology, and the sequences are listed in Table S1. First, 100 μg of (amino)*n*-DNA was dissolved in 100 μL of carbonate buffer (Na<sub>2</sub>CO<sub>3</sub> 9.4 mM, NaHCO<sub>3</sub> 40.7 mM, pH = 9.8). Next, 1.5 mg of S-2-(4-isothiocyanatobenzyl)-diethylenetriaminepentaacetic acid (SCN-DTPA) was added into the solution, and the mixture solution was incubated at 47 °C for 120 min. Subsequently, the (DTPA)*n*-DNA conjugates were purified by the centrifugal filter (3 K, Amicon Ultra) and washed twice with 500 mM sodium acetate buffer (pH 5.8) in the spin filter, combined with 10 mM Ln<sup>3+</sup> metal ions, 5 mM DBCO-Mal linker, and incubated for 4 h at 37 °C. Then, the (Ln<sup>3+</sup>)*n*-DNA tags, which contain a maleimide group at the 3' terminus, were purified by the centrifugal filter (10 K, Amicon Ultra) and washed twice with 100 mM PBS (pH 7.0) buffer in the spin filter. Finally, (Ln<sup>3+</sup>)*n*-DNA tags were determined with

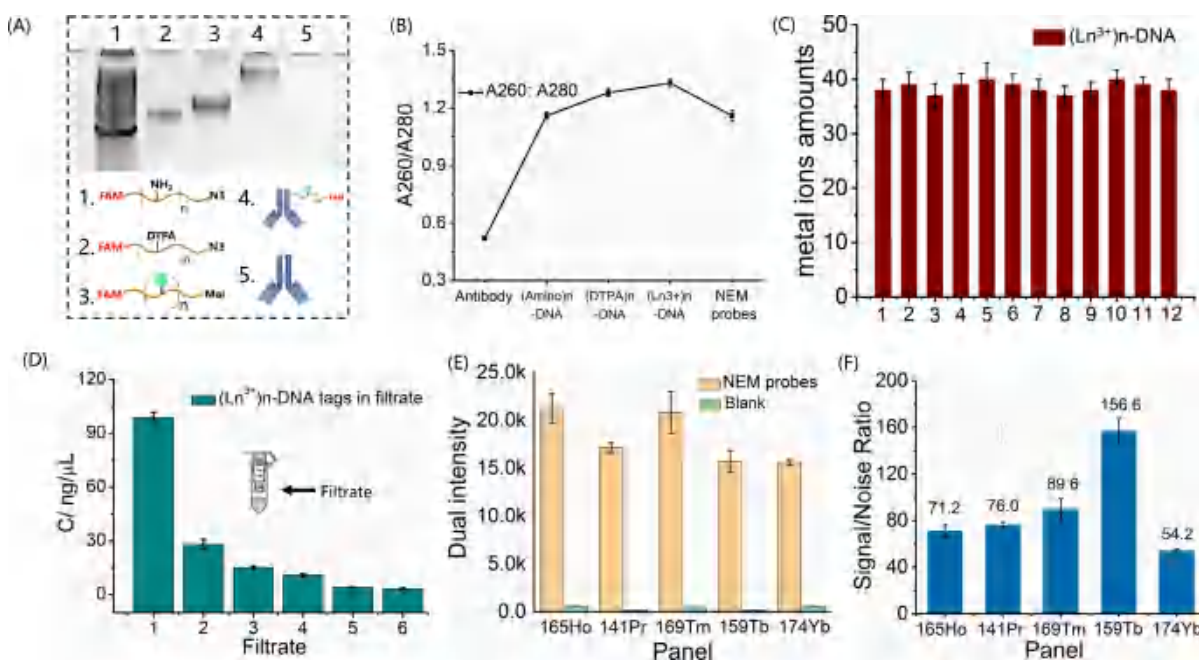


**Figure 1.** Purification and characterization of  $(\text{Ln}^{3+})_n$ -DNA tags and NEM probes. (A) Polyacrylamide gel electrophoresis analysis. (B) A260/A280 ratio of  $(\text{Ln}^{3+})_n$ -DNA tags and NEM probes. (C) Gauging the lanthanide content in  $(\text{Ln}^{3+})_n$ -DNA tags by ICP-MS. The  $(\text{Ln}^{3+})_n$ -DNA tag from 1 to 12 was loaded with 141 Pr, 151 Eu, 153Eu, 159Tb, 161 Dy, 162 Dy, 163 Dy, 165 Ho, 169 Tm, 170 Er, 174 Yb, and 175 Lu. (D) Quantification of the residual  $(\text{Ln}^{3+})_n$ -DNA from the filtrate during the washing steps. (E,F) Mass signal intensity (E) and signal/noise ratio (F) of NEM probes. The error bars from panels (B) to (F) were means  $\pm$  SD for three replicates.

a Nano-800 (Shanghai JP Analytical Instrument Co., Ltd.) spectrophotometer and stored at  $-80\text{ }^\circ\text{C}$ .

**Labeling Antibodies with  $(\text{Ln}^{3+})_n$ -DNA Tags.** Antibodies were labeled with  $(\text{Ln}^{3+})_n$ -DNA tags according to the following protocols. Antibodies were first treated using 5 mM tris (2-carboxyethyl) phosphine hydrochloride (TCEP) in 100 mM PBS buffer (pH 7.0). After incubating at  $37\text{ }^\circ\text{C}$  for 30 min, the antibodies were separated from TCEP with a centrifugal filter (30 K, Amicon Ultra). Then, about 10-fold excess amounts of  $(\text{Ln}^{3+})_n$ -DNA tags were added to the antibodies and incubated for 120 min at  $37\text{ }^\circ\text{C}$ . The  $(\text{Ln}^{3+})_n$ -DNA tagged antibodies, denoted as NEM probes, were subsequently washed six times with the 100 mM PBS buffer (pH 7.0) in the centrifugal filter (100 K, Amicon Ultra). Collecting the filtrate was collected in the centrifuge tube and the NEM probes in the filter. Then, the filtrate was determined with the Nano-800 spectrophotometer and stored at  $4\text{ }^\circ\text{C}$ . The NEM probes were measured by using a Qubit protein assay (Thermo Fisher). Finally, at least 50% Candor PBS Antibody Stabilization solution was used to dilute NEM probes for long-term storage at  $4\text{ }^\circ\text{C}$ .

For the preparation of commercial polymer mass probes, the antibodies were conjugated with a metal-labeled polymer using the Maxpar $\times$ 8 (Standard BioTools, Inc.) antibody labeling kit, following the manufacturer's instructions. After the conjugation reaction, the polymer mass probes were measured by a Nano-800 spectrophotometer and stored at  $4\text{ }^\circ\text{C}$ .

**Polyacrylamide Gel Electrophoresis Experiment.** The (amino)<sub>n</sub>-DNA, (DTPA)<sub>n</sub>-DNA,  $(\text{Ln}^{3+})_n$ -DNA, and NEM probes were analyzed by 10% polyacrylamide gel electrophoresis. First, 20% APS (50  $\mu\text{L}$ ), TEMED (5  $\mu\text{L}$ ), ddH<sub>2</sub>O (2.5 mL), and 40% MBA (2.5 mL) were added to 5 mL of  $2 \times$  TBE buffer and mixed thoroughly. Next, the mixed solution was poured quickly into the gel mold and the gel comb

inserted to form the sample wells; it was left to stand for about 30 min before removing the gel comb. Finally, the samples were characterized with the 12% polyacrylamide gel in  $1 \times$  TBE buffer at 140 V for 60 min, and the polyacrylamide gels were imaged and analyzed using the Bio-Rad Chemi Doc XRS System.

**Cell Staining with NEM Probes.** The patients' blood samples were provided by the Clinical Diagnosis Laboratory of Beijing Tiantan Hospital, Capital Medical University. This study was approved by the Ethics Committee at the Beijing Tiantan Hospital, Capital Medical University (KY2023-189-03). The PBMCs of the patients were extracted from the blood using the MACSprep PBMC Isolation Kit (NovoBiotechnology Co.Ltd.). The PBMCs of healthy people were provided by Milestone Biotechnologies (P123110518C). The suspension of MCF-7 cells was centrifuged to remove the trypsin and disperse the cells in the PBS. The suspension of Jurkat T cells and PBMCs was harvested by centrifugation and dispersed in the PBS. Three million MCF-7 cells, Jurkat T cells, or PBMCs were washed with 4 mL of cell-staining buffer (CSB) and suspended in 100  $\mu\text{L}$  of CSB containing 1  $\mu\text{L}$  of Human TruStain FcX. After 15 min of incubation at room temperature, 2.0  $\mu\text{g}$  of NEM probes or 0.5  $\mu\text{g}$  of commercial polymer mass probes were added and incubated for 30 min. Subsequently, the cells were washed twice with washing buffer by centrifugation to remove the excess NEM probes. Then, cells were stained with an iridium DNA intercalator for 60 min. Finally, the cells were washed with CSB twice and then washed with a cell acquisition solution twice and analyzed with MSFLO mass cytometry (POWCLIN Medical Technology, Hangzhou).

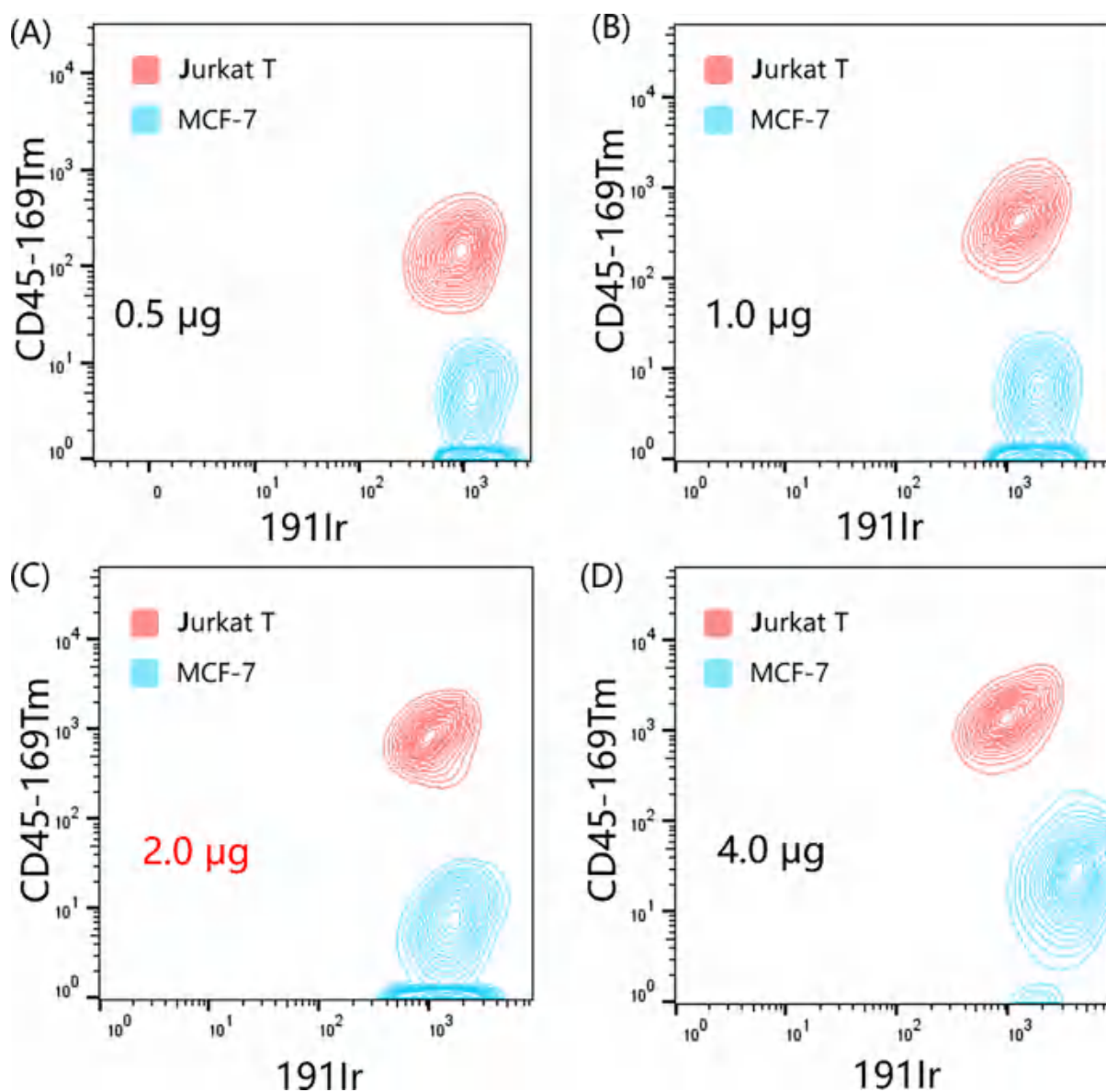


**Figure 2.** Optimization of the NEM probe dosage in the cell-staining assay. The NEM probe dosages used in the cell-staining assay are (A) 0.5  $\mu\text{g}$ , (B) 1.0  $\mu\text{g}$ , (C) 2.0  $\mu\text{g}$ , and (D) 4.0  $\mu\text{g}$ .

## RESULTS AND DISCUSSION

**Synthesis of NEM Probes.** The synthesis and cell staining of NEM probes for mass cytometry are illustrated in [Scheme 1](#). Initially, we designed and synthesized (amino) $_n$ -DNA oligonucleotides enriched with amine modifications and a diazo group at the 3' terminus, as detailed in [Table S1](#). We chose SCN-DTPA, a derivative of DTPA, as the metal-chelating ligand due to its high affinity for lanthanide metals and low exchange rate. The SCN-DTPA ligand was condensed with the amino groups of (amino) $_n$ -DNA ([Scheme 1A](#)). To facilitate antibody binding, (DTPA) $_n$ -DNA was reacted with a DBCO-Mal linker via a click reaction, yielding maleimide-functionalized (Ln $^{3+}$ ) $_n$ -DNA tags ([Scheme 1B](#)). Then, (Ln $^{3+}$ ) $_n$ -DNA tags are conjugated to antibodies via a maleimide–thiol reaction, resulting in the formation of stable Ln $^{3+}$  metal ion-tagged NEM probes ([Scheme 1C](#)). Finally, the cells were stained with NEM probes ([Scheme 1D](#)) and analyzed by MSFLO mass cytometry (POWCLIN, China).

**Purification and Characterization of (Ln $^{3+}$ ) $_n$ -DNA Tags and NEM Probes.** First, we characterized (Ln $^{3+}$ ) $_n$ -DNA tags and verified their composition by polyacrylamide gel electrophoresis, a spectrophotometer, and ICP-MS analysis. As shown in [Figure 1A](#), the electrophoretic mobility of (DTPA) $_n$ -DNA and (Ln $^{3+}$ ) $_n$ -DNA on the polyacrylamide gel demonstrated a slight reduction compared to that of (amino) $_n$ -DNA, indicating successful tagging. Then, we also used the Nano-800 spectrophotometer to evaluate the products at each stage. The absorbance ratio between 260 and 280 nm (A $_{260}$ /A $_{280}$ ) serves as a critical metric for assessing the purity of DNA or antibodies. Following the conjugation with SCN-DTPA and the DBCO-Mal linker, the A $_{260}$ /A $_{280}$  ratio of (Ln $^{3+}$ ) $_n$ -DNA exhibited significant shifts ([Figure 1B](#)), confirming effective conjugation of the components to (amino) $_n$ -DNA. Finally, the lanthanide content of the (Ln $^{3+}$ ) $_n$ -DNA tags was quantified by ICP-MS, revealing an average of  $38 \pm 3$  lanthanides per (Ln $^{3+}$ ) $_n$ -DNA molecule ([Figure 1C](#)). Besides, there is good repeatability between different experiments, and the loading

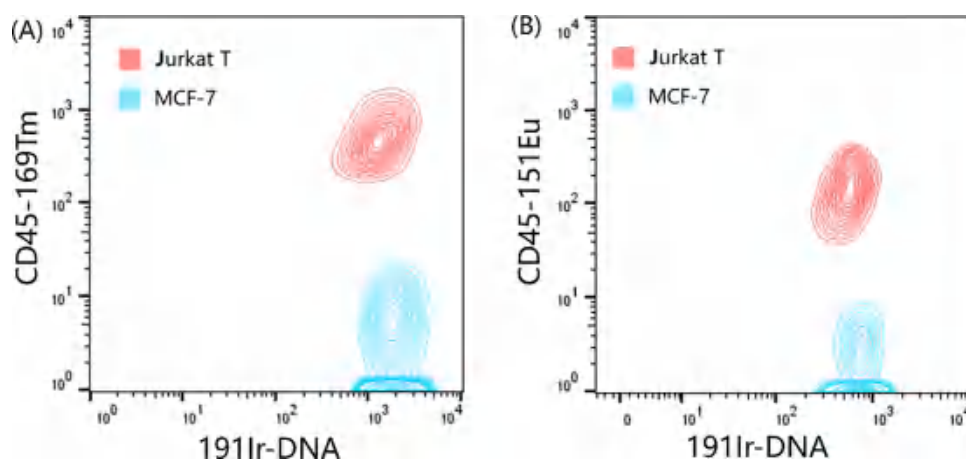


Figure 3. Mass cytometry of the MCF-7 and Jurkat T cells by staining with (A) NEM probes and (B) commercial polymer mass probes.

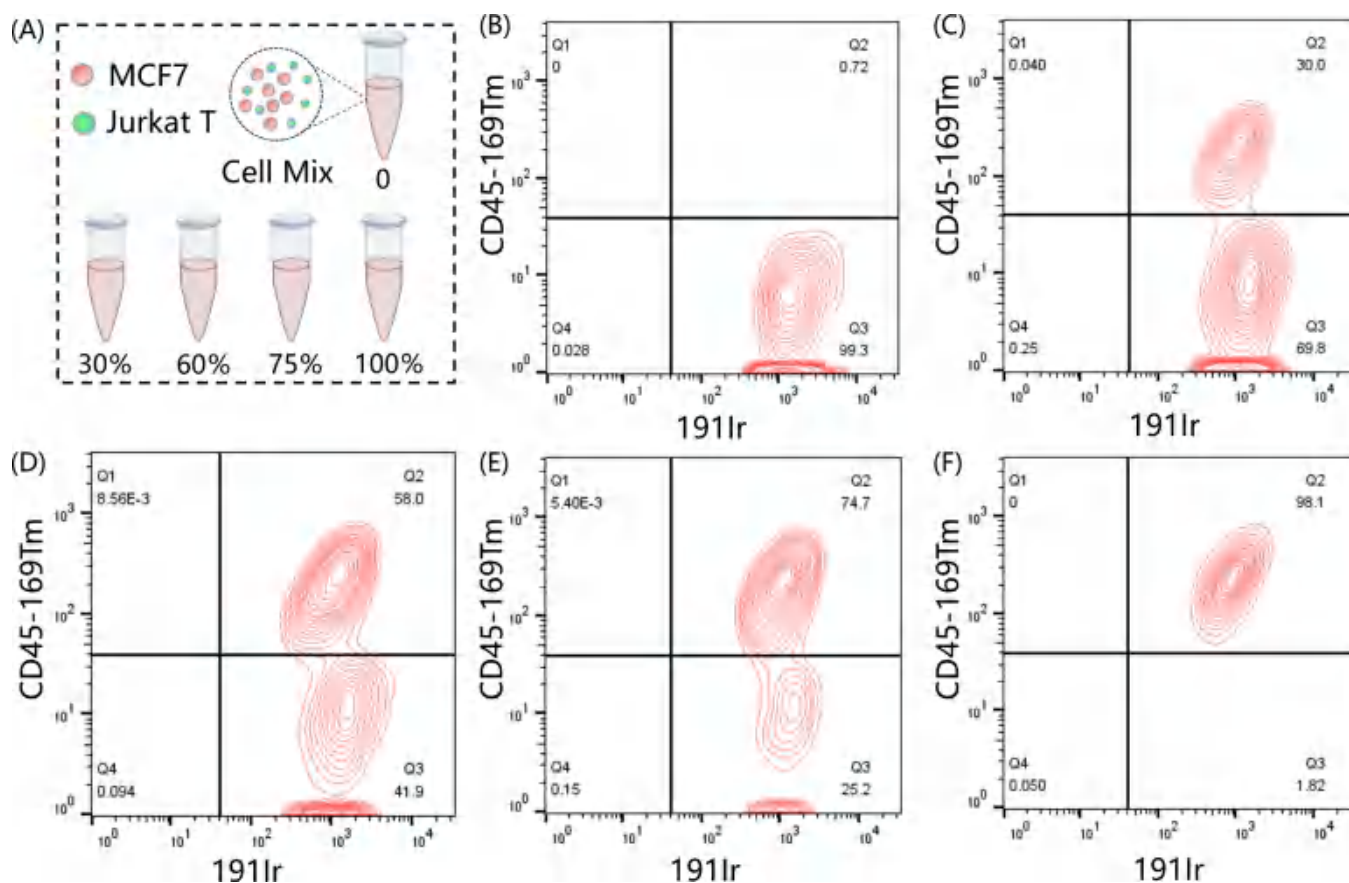
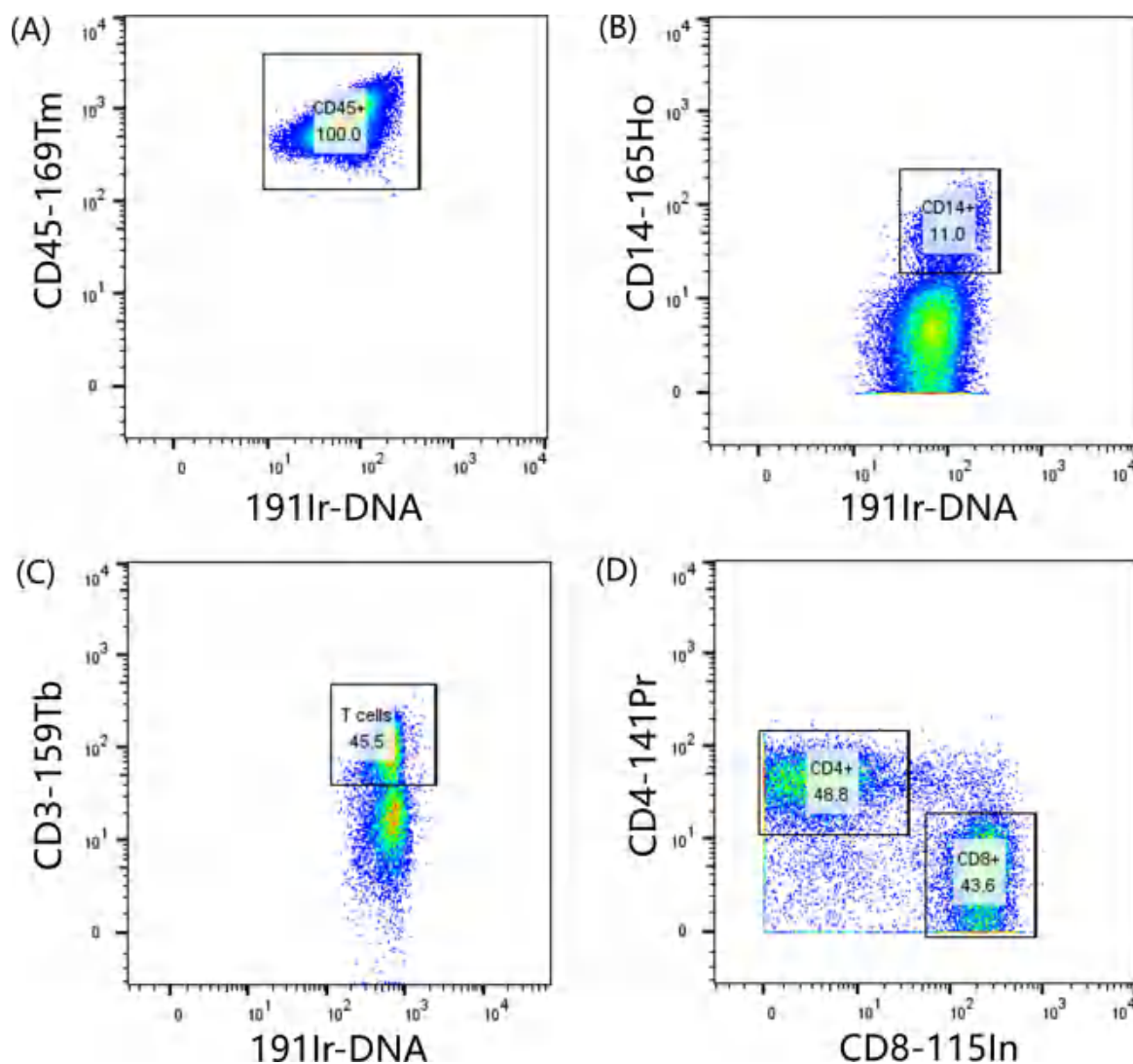


Figure 4. Titration of MCF-7/Jurkat T cell mixtures using NEM probes with mass cytometry. (A) Preparation of MCF-7/Jurkat T cell mixtures. (B–F) The mass cytometry analysis of the cell mixtures was done by using NEM probes. The Jurkat T cell population is (B) 0, (C) 0.3, (D) 0.6, (E) 0.75, and (F) 1 million, respectively. Q2 represents Jurkat T cells, and Q3 represents MCF-7 cells.

rate of  $\text{Ln}^{3+}$  metal atoms is not affected by the type of lanthanides.

To purify the NEM probes from unreacted  $(\text{Ln}^{3+})_n$ -DNA tags, we subsequently washed the NEM probes six times in the centrifugal filter. Figure 1D illustrates that with each washing cycle, the concentration of residual  $(\text{Ln}^{3+})_n$ -DNA in the filtrate progressively diminished. Upon completion of five washing cycles, the A260/A280 ratio of the filtrate is the same as that of the NEM probes (Figure S1A). A notable decrease in the mobility of NEM probes observed in Figure 1A further confirms the successful conjugation of  $(\text{Ln}^{3+})_n$ -DNA to

antibodies and the substantial removal of unreacted tags. Additionally, to further measure the batch-to-batch consistency metrics, the NEM probe was analyzed by size exclusion chromatography. As shown in Figure S1B, the chromatographic peak of the NEM probe could be clearly separated from that of the antibody. Moreover, the peak shapes of NEM probes from the two batches almost completely overlapped. Therefore, the batch-to-batch consistency metrics of the NEM probe are good. Then, the NEM probes were quantified with the Qubit protein assay (Thermo Fisher), and the lanthanide content of each NEM probe was analyzed by ICP-MS (Figure



**Figure 5.** Feasibility of NEM probes in multiplexed detection of different biomarkers in PBMCs. (A) CD45+ cell populations from PBMCs. (B,C) Discriminated monocytes (CD14+) and T (CD3+) cell populations from CD45+ PBMCs. (D) Distinguish CD4+ and CD8+ T cell populations from T (CD3+) cells.

(S1C,D). The result showed that the yield is approximately 40–50%, and each NEM probe can bind  $210 \pm 20$  metal ions. Then, it can be inferred that each probe was bound with approximately five or six DNA tags. To evaluate the versatility of this design for making different lanthanide metal ion-tagged NEM probes, five different lanthanide ions ( $\text{Tb}^{3+}$ ,  $\text{Pr}^{3+}$ ,  $\text{Yb}^{3+}$ ,  $\text{Ho}^{3+}$ , and  $\text{Tm}^{3+}$ ) were used to prepare five NEM probes (CD3, CD4, CD19, CD14, and CD45), respectively. We diluted  $0.5 \mu\text{g}$  of each NEM probe into 1 mL of 3%  $\text{HNO}_3$  solution and tested their mass signal intensity by ICP-MS. As shown in Figure 1E,F, the NEM probes demonstrated strong performance, and the mass signal/noise ratio of the five NEM probes is above 50.

**Validation of NEM Probes by Mass Cytometry.** To evaluate the performance of the NEM probes in mass cytometry, MCF-7 breast cancer cells and Jurkat T cells were chosen as the model system. CD45, prominently expressed on Jurkat T cells, was targeted as the biomarker, while MCF-7 cells, which lack CD45 expression, served as a negative internal control. To reduce the nonspecific adsorption of the NEM probes, we initially investigated various washing buffers in the

staining step. As depicted in Figure S2, the washing buffer has a significant impact on the experiment. The Stellaris RNA Fish wash buffer and sodium citrate buffer have the best cleaning effects compared to those of CSB and sodium citrate buffer containing 5% formamide. Due to its cost-effectiveness, the sodium citrate buffer was used as the washing buffer for the subsequent experiments. Subsequently, we optimized the amounts of NEM probes in the cell-staining assay. With the increase in NEM probe dosage, the mean mass intensity of Jurkat T cells increased gradually (Figure 2A–D). However, when the dosage is  $4.0 \mu\text{g}$ , the mean mass intensity of MCF-7 cells increased immediately due to the nonspecific adsorption. Therefore,  $2.0 \mu\text{g}$  is optimal for the proposed assay.

Under optimum experimental conditions, we compared the performance of NEM probes with commercial polymer mass probes and double-stranded DNA mass probes produced by PCR (see the sequence in Table S1). As depicted in Figure 3 and Table S2, the mean mass intensity ratio of Jurkat T cells to MCF-7 cells (J/M ratio) from NEM probes was 200.91, which was higher than that of the commercial probe (97.71). Meanwhile, the coefficient variations of Jurkat T cells and

MCF-7 cells are 45.70 and 106.82, respectively, both of which were smaller than those of the commercial probes (88.73 for T cells and 135.12 for MCF-7 cells). Besides, by comparing Figure 3A and Figure S3, the J/M ratio from the NEM probes is much better than that from the double-strand DNA mass probes. Due to the nonspecific adsorption of free double-strand DNA mass tags in the double-strand DNA mass probes, the background signal of the double-strand DNA mass probe is much higher than that of the NEM probe. These results indicated that the NEM probes offer better discrimination of the cells and higher sensitivity.

Next, we further investigated the quantitative detection ability of NEM probes by using MCF-7/Jurkat T cell mixtures. The total cell count in each mixture was maintained at 1 million, while the proportion of Jurkat T cells was varied across several conditions: 0, 0.3, 0.6, 0.75, and 1 million (Figure 4A). Figure 4B–F demonstrates a corresponding increase in the positive peak for T cells as the proportion of Jurkat T cells increased. This pattern confirms that NEM probes can quantitatively assess specific cell populations, underscoring their utility in precise cellular analysis.

Given that mass cytometry is widely employed for the multiplexed detection of various biomarkers, we evaluated the feasibility of NEM probes in a multiplexed assay using PBMCs. PBMCs were stained with a panel of five NEM probes (CD3-159Tb, CD4-141Pr, CD8-115In, CD14-165Ho, and CD45-169Tm). As illustrated in Figure 5, distinct cell populations, including monocytes, CD3+ T cells, CD4+ T cells, and CD8+ T cells, were successfully discriminated, with results comparable to fluorescence flow cytometry and the commercial polymer mass probes (Table S3). These findings highlight the potential of NEM probes for multiparametric cellular analysis. According to Figure S4, the mass signal intensity of the probes remained stable after 40 days of storage at 4 °C, demonstrating their robust stability.

Finally, the NEM probes were applied in multiplex clinical diagnoses of different CD markers in PBMCs from patients suffering from demyelinating diseases, neuromyelitis optica spectrum disorders (NMOSDs), and acute myeloid leukemia, respectively. As shown in Table S4, compared with healthy individuals, the proportion of CD3+ T cells from these three patients is significantly increased, while the proportion of B lymphocytes (CD3- CD19+) is remarkably decreased. In addition, in patients with NMOSD and acute myeloid leukemia, the proportion of CD3+ and CD4+ cells increases. In contrast, in patients with demyelinating diseases, the proportion of CD3+ CD8+ cells increases. These results were consistent with those of the Agilent fluorescence flow cytometry detection kit (Table S5).

## CONCLUSIONS

In conclusion, we successfully developed NEM probes based on the nucleotide backbone, demonstrating their utility in mass cytometry for the detection of specific cell-surface biomarkers. Nevertheless, the higher metal-loading capacity of the NEM probes enabled them to achieve comparable or higher sensitivity and mean mass intensity compared with commercially available mass probes. What's more, the NEM probes have been successfully used in multiplex clinical diagnosis of different CD markers in patients' PBMCs. We postulate that NEM probes have strong potential for broad clinical diagnosis and will drive advancements in multiplexed cell analysis.

## ASSOCIATED CONTENT

### Supporting Information

The Supporting Information is available free of charge at <https://pubs.acs.org/doi/10.1021/acs.analchem.5c01011>.

Materials and reagents; sequences of (amino)<sub>n</sub>-DNA and the double-stranded DNA tag; characterization of NEM probes by size exclusion chromatography and ICP-MS; optimization of the washing buffer; comparison of the performance of NEM probes with polymer mass probes; stability of NEM probes; and the performance of NEM probes in multiplexed detection of PBMCs from patients and healthy people (PDF)

## AUTHOR INFORMATION

### Corresponding Authors

**Zhian Hu** – School of Chemistry and Biological Engineering, University of Science and Technology Beijing, Beijing 100083, China; [orcid.org/0000-0002-4475-1477](https://orcid.org/0000-0002-4475-1477); Email: [zhianhu@ustb.edu.cn](mailto:zhianhu@ustb.edu.cn)

**Gongwei Sun** – Division of Chemical Metrology and Analytical Science, National Institute of Metrology, Beijing 100029, China; Email: [sungw@nim.ac.cn](mailto:sungw@nim.ac.cn)

**Sichun Zhang** – Department of Chemistry, Tsinghua University, Beijing 100084, China; State Key Laboratory of Analytical Chemistry for Life Science, School of Chemistry and Chemical Engineering, Nanjing University, Nanjing 210093, China; [orcid.org/0000-0001-8927-2376](https://orcid.org/0000-0001-8927-2376); Email: [sczhang@mail.tsinghua.edu.cn](mailto:sczhang@mail.tsinghua.edu.cn)

### Authors

**Weiliang Liu** – Department of Chemistry, Tsinghua University, Beijing 100084, China; [orcid.org/0000-0002-4281-0541](https://orcid.org/0000-0002-4281-0541)

**Wencan Jiang** – Department of Clinical Diagnosis, Laboratory of Beijing Tiantan Hospital and Capital Medical University, Beijing 100070, China

**Jinhui Liu** – Department of Chemistry, Tsinghua University, Beijing 100084, China; [orcid.org/0000-0003-2052-877X](https://orcid.org/0000-0003-2052-877X)

**Xinrong Zhang** – Department of Chemistry, Tsinghua University, Beijing 100084, China

Complete contact information is available at:

<https://pubs.acs.org/10.1021/acs.analchem.5c01011>

### Author Contributions

Weiliang Liu: writing (review and editing), methodology, data curation. Zhian Hu: writing (review and editing), methodology, investigation, funding acquisition. Jinhui Liu and Wencan Jiang: validation, data curation. Gongwei Sun: validation, data curation, funding acquisition. Sichun Zhang and Xinrong Zhang: project administration, funding acquisition. All authors discussed the results and implications and commented on the manuscript at all stages.

### Notes

The authors declare no competing financial interest.

## ACKNOWLEDGMENTS

We acknowledge the support by National Science and Technology Major Project of the Ministry of Science and Technology of China (2022YFF0710200); the Postdoctoral Fellowship Program (Grade C) of China Postdoctoral Science Foundation (GZC20231252); the NIM Research Project

(AKYZZ2447); the National Natural Science Foundation of China (22304007, 82202623, and 22404093); Beijing Municipal Natural Science Foundation No. 2252014, and Open Research Fund of State Key Laboratory of Analytical Chemistry for Life Science, School of Chemistry and Chemical Engineering, Nanjing University.

## REFERENCES

- (1) Majonis, D.; Herrera, I.; Ornatsky, O.; Schulze, M.; Lou, X. D.; Soleimani, M.; Nitz, M.; Winnik, M. A. *Anal. Chem.* **2010**, *82* (21), 8961–8969.
- (2) Frei, A. P.; Bava, F. A.; Zunder, E. R.; Hsieh, E. W. Y.; Chen, S. Y.; Nolan, G. P.; Gherardini, P. F. *Nat. methods* **2016**, *13* (3), 269.
- (3) Abdelrahman, A. I.; Dai, S.; Thickett, S. C.; Ornatsky, O.; Bandura, D.; Baranov, V.; Winnik, M. A. *J. Am. Chem. Soc.* **2010**, *132* (7), 2465–2465.
- (4) Cossarizza, A.; Chang, H. D.; Radbruch, A.; Acs, A.; Adam, D.; Adam-Klages, S.; Agace, W. W.; Aghaeepour, N.; Akdis, M.; Allez, M.; et al. *Eur. J. Immunol.* **2019**, *49* (10), 1457–1973.
- (5) Newell, E. W.; Davis, M. M. *Nat. Biotechnol.* **2014**, *32* (2), 149–157.
- (6) Bendall, S. C.; Simonds, E. F.; Qiu, P.; Amir, E. A. D.; Krutzik, P. O.; Finck, R.; Bruggner, R. V.; Melamed, R.; Trejo, A.; Ornatsky, O. I.; et al. *Science* **2011**, *332* (6030), 687–696.
- (7) Atkuri, K. R.; Stevens, J. C.; Neubert, H. *Drug Metab. Dispos.* **2015**, *43* (2), 227–233.
- (8) Kingsmore, S. F. *Nat. Rev. Drug Discovery* **2006**, *5* (4), 310–320.
- (9) Sun, G. W.; Liu, W. L.; Liu, J. H.; Sheng, L. F.; Xing, Z.; Zhang, S. C.; Zhang, X. R. *At. Spectrosc.* **2023**, *44* (6), 392–400.
- (10) Han, G. J.; Spitzer, M. H.; Bendall, S. C.; Fantl, W. J.; Nolan, G. P. *Nat. Protoc.* **2018**, *13* (10), 2121–2148.
- (11) Maecker, H. T.; Lindstrom, T. M.; Robinson, W. H.; Utz, P. J.; Hale, M.; Boyd, S. D.; Shen-Orr, S. S.; Fathman, C. G. *Nat. Rev. Rheumatol.* **2012**, *8* (10), 317–328.
- (12) Lou, X. D.; Zhang, G. H.; Herrera, I.; Kinach, R.; Ornatsky, O.; Baranov, V.; Nitz, M.; Winnik, M. A. *Angew. Chem.-Int. Ed.* **2007**, *46* (32), 6111–6114.
- (13) Jabbour, E.; Kantarjian, H. *Am. J. Hematol.* **2018**, *93* (3), 442–459.
- (14) Al-mafragy, H. S.; Al-awade, H. A. R. *J. Pharm. Sci. Res.* **2020**, *195*.
- (15) Malile, B.; Brkic, J.; Bouzekri, A.; Wilson, D. J.; Ornatsky, O.; Peng, C.; Chen, J. I. L. *ACS Appl. Bio Mater.* **2019**, *2* (10), 4316–4323.
- (16) Newell, E. W.; Sigal, N.; Bendall, S. C.; Nolan, G. P.; Davis, M. M. *Immunity* **2013**, *198*.
- (17) Horowitz, A.; Strauss-Albee, D. M.; Leipold, M.; Kubo, J.; Nemat-Gorgani, N.; Dogan, O. C.; Dekker, C. L.; Mackey, S.; Maecker, H.; Swan, G. E.; et al. *Sci. Transl. Med.* **2013**, *5*, 208.
- (18) Wu, X.; DeGottardi, Q.; Wu, I. C.; Yu, J. B.; Wu, L.; Ye, F. M.; Kuo, C. T.; Kwok, W. W.; Chiu, D. T. *Angew. Chem.-Int. Ed.* **2017**, *56* (47), 14908–14912.
- (19) Pichaandi, J.; Tong, L.; Bouzekri, A.; Yu, Q.; Ornatsky, O.; Baranov, V.; Winnik, M. A. *Chem. Mater.* **2017**, *29* (11), 4980–4990.
- (20) Pichaandi, J.; Zhao, G. Y.; Bouzekri, A.; Lu, E.; Ornatsky, O.; Baranov, V.; Nitz, M.; Winnik, M. A. *Chem. Sci.* **2019**, *10* (10), 2965–2974.
- (21) Dang, J.; Li, H.; Zhang, L.; Li, S.; Zhang, T.; Huang, S.; Li, Y.; Huang, C.; Ke, Y.; Shen, G.; Zhi, X.; Ding, X.; et al. *Adv. Mater.* **2021**, *33*, 35.
- (22) Arnett, L. P.; Rana, R.; Chung, W. W. Y.; Li, X. C.; Abtahi, M.; Majonis, D.; Bassan, J.; Nitz, M.; Winnik, M. A. *Chem. Rev.* **2023**, *123* (3), 1166–1205.
- (23) Hu, Z.; Sun, G. W.; Jiang, W. C.; Xu, F. J.; Zhang, Y. Q.; Xia, M. C.; Pan, X. Y.; Xing, Z.; Zhang, S. C.; Zhang, X. R. *Anal. Chem.* **2019**, *91* (9), 5980–5986.